

FIRST PROTOTYPE FOR SURFACE ALBEDO RETRIEVAL BASED ON SENTINEL-3 OLCI AND SLSTR DATA IN THE FRAMEWORK OF COPERNICUS CLIMATE CHANGE SERVICE

Jorge Sánchez-Zapero ^{1,*}, Fernando Camacho ¹, Jonathan León-Tavares ², Enrique Martínez-Sánchez ¹, Javier Gorroño ¹, Iskander Benhadj ², Carolien Toté ², Else Swinen ² and Joaquín Muñoz-Sabater ³

¹ Earth Observation Laboratory (EOLAB), Parc Científic Universitat de València, C/ Catedrático Agustín Escardino 9, 46980 Paterna (Valencia), Spain.

² Flemish Institute for Technological Research (VITO), Remote Sensing Unit, Boeretang 200, B-2400 Mol, Belgium; iskander.benhadj@vito.be

³ European Centre for Medium-Range Weather Forecasts (ECMWF), Shinfield Road, RG2 8JD, Reading, UK; joaquin.Munoz@ecmwf.int

* Correspondence: jorge.sanchez@eolab.es; Tel.: +34-963-769-448

KEY WORDS: C3S, Surface Albedo, Sentinel-3, OLCI, SLSTR, algorithm

ABSTRACT

This work describes the different algorithmic steps used to retrieve the first Surface Albedo (SA) product based on Sentinel-3 (S-3) data in the framework of the Copernicus Climate Change Service (C3S). The atmospherically corrected Top-Of-Atmosphere (TOA) reflectances into Top-Of-Canopy (TOC) reflectances are brokered from Copernicus Global Land Service (CGLS). The BRDF inversion model transforms the TOC reflectances into model coefficients. Next, the spectral and angular integration steps are implemented, which take the latter coefficients as input to produce spectral and broadband albedo quantities.

The preliminary validation of BSA broadband albedo for the total shortwave shows good overall spatio-temporal consistency with C3S PROBA-V SA products, and good spatial consistency with MCD43A3 C6 over the Iberian Peninsula (mean bias lower than 5%), with some underestimation of snow targets.

1. INTRODUCTION

The C3S mission is to produce Climate Data Records (CDR) of many essential climate variables, among them the SA which quantifies

the fraction of solar energy reflected by the surface of the Earth.

The most relevant albedo quantity for applications related to the energy budget refers to the total short-wave domain (SW: [0.3 μ m, 4 μ m]), comprising the visible (VIS: [0.4 μ m, 0.7 μ m]) and near infrared (NIR: [0.7 μ m, 4 μ m]) wavelength ranges, where the solar downwelling radiation dominates.

2. ALGORITHM DESCRIPTION

The current prototype of the SA retrieval algorithm incorporates measurements from OLCI and SLSTR instruments onboard S-3 A and B satellites. Several steps are required to transform TOA reflectance values from both sensors into broadband albedo values. First, the atmospheric correction module transforms TOA into TOC reflectance. Then, the BRDF inversion module produces model coefficients that are then used by the spectral integration module to generate spectral albedo quantities for the selected S-3 OLCI and bands. The Black-Sky Albedo (BSA) and White-Sky Albedo (WSA) are calculated in this step. At last, the angular integration module infers broadband albedo quantities for three standard broad bands (VIS, NIR and SW). Such

approach was adopted for retrieving the albedo products in near-real time derived from POLDER (Leroy et al., 1997), MODIS MCD43 (Schaaf et al., 2002; Strahler et al., 1999), and SEVIRI (Carrer et al., 2010; Geiger et al., 2008) in the framework of the LSA SAF. Same approach applied in the framework of the LSA SAF was later adapted to SPOT/VGT and PROBA-V in CGLS and C3S.

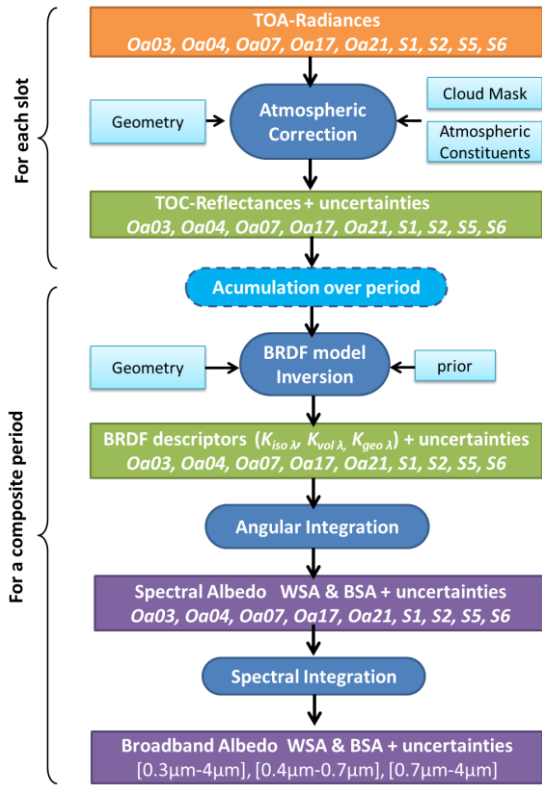


Figure 1: Flow diagram of the S-3 SA retrieval algorithm and the corresponding modules.

2.1. S-3 TOC-r input data

The atmospherically corrected reflectances are brokered from CGLS S-3 pre-processing chain, that consists in the following steps: (1) collocation and reprojection of OLCI and SLSTR Level1B input on the regular PROBA-V 300m grid using the S3-MPC SYN_L1C tool; (2) cloud, snow and cloud shadow detection based on OLCI Idepix and SLSTR summary cloud flag; (3) atmospheric correction based on SMAC.

Table 1: S-3 OLCI (Oa03, Oa04, Oa07, Oa17 and Oa21) and SLSTR (S1, S2, S5 and S6) spectral bands used as input for the SA retrieval.

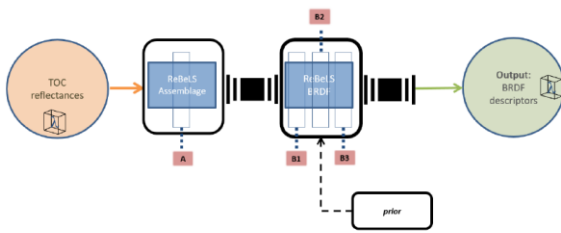
OLCI band	Oa03	Oa04	Oa07	Oa17	Oa21
λ_{centre} (nm)	442.5	490	620	865	1020
SLSTR band	S1	S2	S5	S6	
λ_{centre} (nm)	554.27	659.47	1613.4	2255.7	

There are 20 spectral OLCI and SLSTR bands from CGLS available. The bands with little information, bands in highly sensitive areas and/or redundant (SLSTR and OLCI overlaps) have been discarded. The central wavelengths of the selected 9 bands used as the input of the algorithm are summarized in Table 1.

2.2. BRDF descriptors retrieval

The approximation of the BRDF for land surface is achieved by numerical inversion of kernel-driven semi-empirical models (i.e. RossThick-LiSparseReciprocal) (Roujean, 2017). Thus, to constraint the results of the BRDF descriptors retrievals in a realistic fashion, the present algorithm uses a climatology of BRDF descriptors (k_{iso} - Isotropic kernel weight; k_{vol} - Volumetric kernel weight; k_{geo} - Geometric kernel weight) built from prior MODIS MCD43A1 and MCD43A2 (Strahler et al., 1999) products.

Three main stages are involved in the retrieval of BRDF descriptors (see Figure 2): A (Assemblage), B1 (BRDF model), B2 (Inversion) and B3 (Quality control).



- **A – Assemblage:** Accumulation of observations over a selected period of time. Using information from quality indicators, only clear observations are retained for further processing.
- **B1 – BRDF model:** Kernels from a semi-empirical BRDF model are computed for each observation
- **B2 – Inversion:** BRDF descriptors that best represent the ensemble of observations are found by solving an inverse problem with the addition of regularisation (prior).
- **B3 – Quality control:** A quality information layer is assembled to reflect availability of observations and whether (or not) the BRDF model inversion was successful.

Figure 2: Flow diagram of the BRDF retrieval algorithm correction algorithm. See inner caption for a brief explanation of each stage.

2.3. Angular integration

The angular integration of Bidirectional Reflectance Factor (BRF) over all the viewing angles is required to calculate the BSA and WSA. Instead of directly calculating the integral, the same polynomial method proposed in the MODIS albedo estimating procedure (Strahler et al., 1999) is used, as the BRDF model inversion uses the same semi-empirical kernel-based reflectance model.

2.4. Spectral integration

Broadband albedo is defined as the integral of spectral albedo over a certain wavelength interval weighted by the spectral irradiance. Since the integral can be approximated as a weighted sum of the integrand at discrete values of the integration variable, broadband albedo may be expressed as a linear combination of the spectral albedo values in the available spectral bands. Previous works (e.g. MCD43A3), converts the spectral albedo by applying a linear regression over a set of spectral albedo against its respective broadband albedo (Geiger et al., 2008; Liang, 2001). A set of coefficients is produced for the snow cases and a different set for snow-

free targets in three different broadband ranges (VIS, NIR, SW).

This set of broadband albedo is based on a database of spectral downwelling irradiance and simulated spectral albedo/measured spectral reflectance. The novelty of this algorithm is focused on reconsidering the representativeness of the surface and atmospheric properties that are input to the linear regression, and each biome was weighted in the linear regression according to its global representativeness.

3. C3S SENTINEL-3 SA PRODUCTS

The output products are the spectral and broadband BSA and WSA every 10 days.

XX

XX

XX

XX

XXXXXXXXXX **Insert global map** XXXXXXXXXXXXXXX

Figure 3: Global map of broadband BSA in the total shortwave for yyyy.mm.dd.

4. PRELIMINARY VALIDATION

Two different validation exercises were performed to preliminary evaluate the quality of S-3 SA products. Firstly, good global overall spatio-temporal consistency (linear regression close to 1:1 line and high correlation) was found in comparison with C3S SA PROBA-V products over LANDVAL sites, a representative global network of samples (Sánchez-Zapero et al., 2020) (Figure 4). Secondly, the spatial consistency was evaluated against MODIS MCD43A3 C6 products over the tile located over the Iberian Peninsula (Figure 5), showing mean positive bias lower than 5%, with most of the differences within ±0.05 except some underestimation over snow targets.

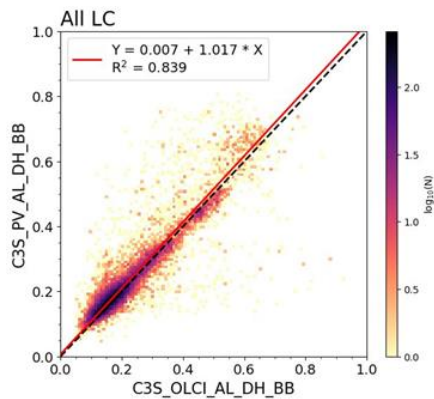


Figure 4: Overall scatter-plots between C3S S-3 SA and PROBA-V SA V2 BSA broadband total SW products for one year of data over LANDVAL sites.

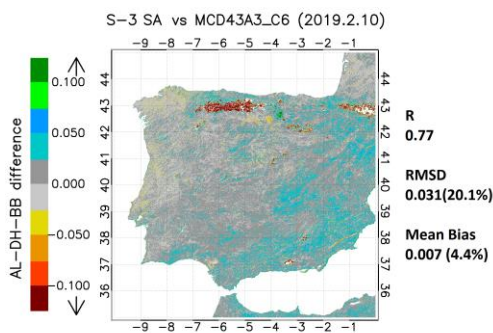


Figure 5: Differences between C3S S-3 SA and MCD43A3 C6 BSA broadband total SW products over the Iberian Peninsula for 10th February, 2019.

5. CONCLUSIONS

These C3S S-3 SA products provide the continuity of the C3S CDR at an improved spatial resolution (300 m). The C3S CDR based on past time series were retrieved from NOAA/AVHRR (April 1981-2005, at 5 km), SPOT/VGT (December 1999 - May 2014, at 1 km) and PROBA-V (December 2013 – June 2020, at 1 km) data. The use of S-3 OLCI and SLSTR also offers richer spectral information compared with previous datasets (nine spectral channels used in S-3 instead of the four channels used in previous products).

REFERENCES

Carrer, D., et al. (2010). Comparing operational MSG/SEVIRI Land Surface albedo products from

- Land SAF with ground measurements and MODIS. *IEEE Transactions on Geoscience and Remote Sensing*, 48(4 PART 1), 1714–1728. <https://doi.org/10.1109/TGRS.2009.2034530>
- Geiger, B., et al (2008). Land surface albedo derived on a daily basis from meteosat second generation observations. *IEEE Transactions on Geoscience and Remote Sensing*, 46(11), 3841–3856. <https://doi.org/10.1109/TGRS.2008.2001798>
- Leroy, M., et al. (1997). Retrieval of atmospheric properties and surface bidirectional reflectances over land from POLDER/ADEOS. *Journal of Geophysical Research Atmospheres*, 102(14), 17023–17037. <https://doi.org/10.1029/96jd02662>
- Liang, S. (2001). Narrowband to broadband conversions of land surface albedo I Algorithms. *Remote Sens. Environ.*, 76(2000), 213–238. [https://doi.org/10.1016/S0034-4257\(00\)00205-4](https://doi.org/10.1016/S0034-4257(00)00205-4)
- Roujean, J. L. (2017). Inversion of lumped parameters using BRDF kernels. In *Comprehensive Remote Sensing* (Vols. 1–9, pp. 23–34). Elsevier. <https://doi.org/10.1016/B978-0-12-409548-9.10346-X>
- Sánchez-Zapero, J., et al. (2020). Quality Assessment of PROBA-V Surface Albedo V1 for the Continuity of the Copernicus Climate Change Service. *Remote Sensing 2020, Vol. 12, Page 2596, 12(16)*, 2596. <https://doi.org/10.3390/rs12162596>
- Schaaf, C. B., e. (2002). First operational BRDF, albedo nadir reflectance products from MODIS. *Remote Sensing of Environment*, 83(1–2), 135–148. [https://doi.org/10.1016/S0034-4257\(02\)00091-3](https://doi.org/10.1016/S0034-4257(02)00091-3)
- Strahler, A. H., Muller, J.-P., & Members, M. S. T. (1999). *MODIS BRDF/Albedo Product: Algorithm Theoretical Basis Document Version 5.0*. [https://lpdaac.usgs.gov/documents/97/MCD43_ATB D.pdf](https://lpdaac.usgs.gov/documents/97/MCD43_ATB_D.pdf)